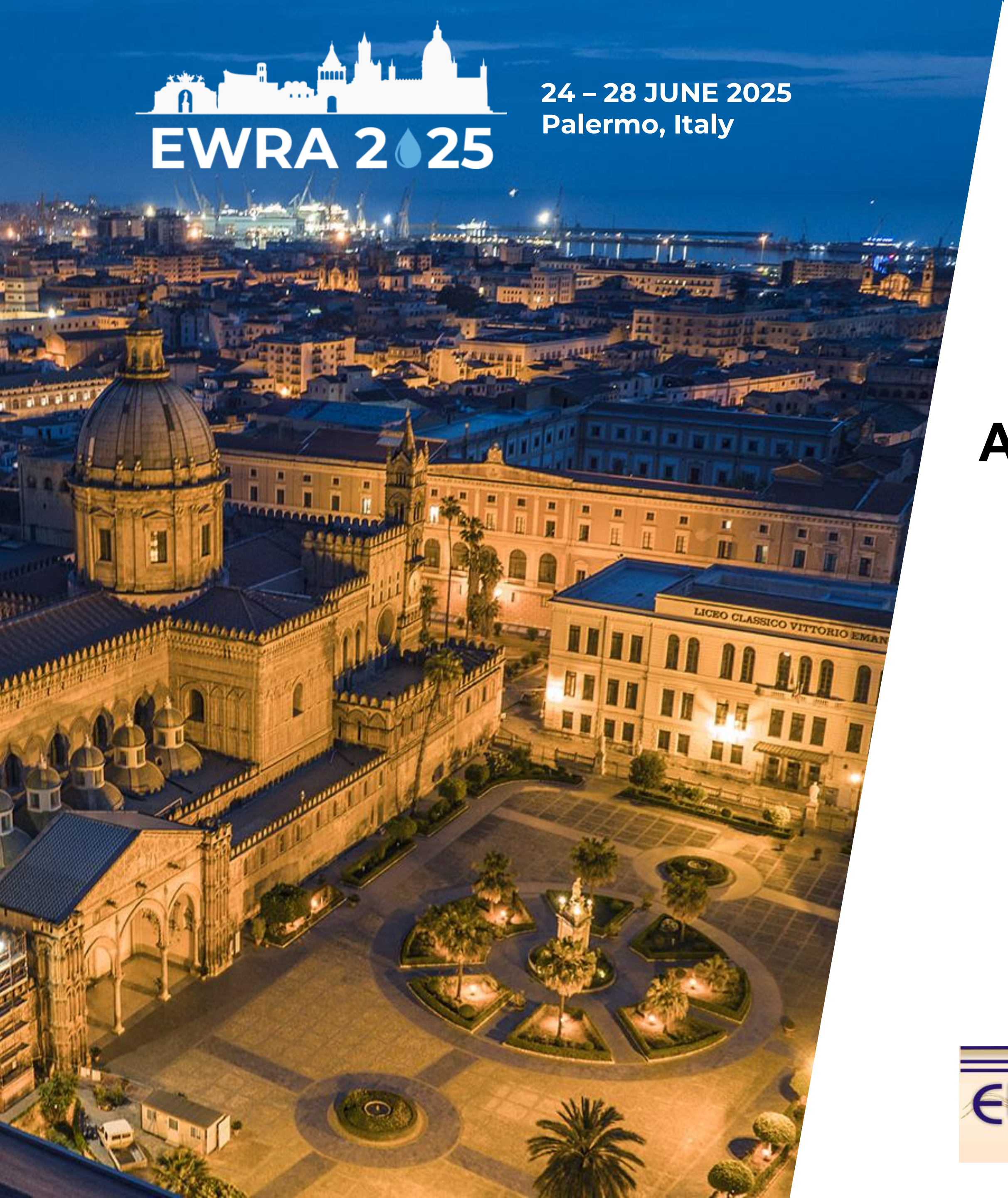

XIII WORLD CONGRESS

of the European Water Resources Association

New challenges in understanding and managing
water-related risks in a changing environment

Analysis of upper dam failure and cascade impacts in pumped-storage hydropower systems: a case study of Brava - Sfikia scheme, Aliakmon River, Greece

P. Dimas[1*], A. Lykou[1], A. Zarkadoulas[1], G.K. Sakki[1],
A. Efstratiadis[1] and C. Makropoulos[1]
[1]Dept. of Water Resources and Environmental Engineering,
School of Civil Engineering, NTUA, Athens, Greece

*Corresponding author email: pdimas@mail.ntua.gr

EWRA

Università degli Studi di Palermo

HYCLIC
Hydrology & Climate Change Impacts Lab

Presentation structure

1. Study objective
2. Study area – technical data
3. Investigation of dam breach scenarios
4. Flood wave propagation between the upper and the lower reservoir
5. Assessment of cascade impacts on the lower reservoir (Routing of the flood hydrograph & impulse wave/tsunami generation)
6. Conclusions
7. References

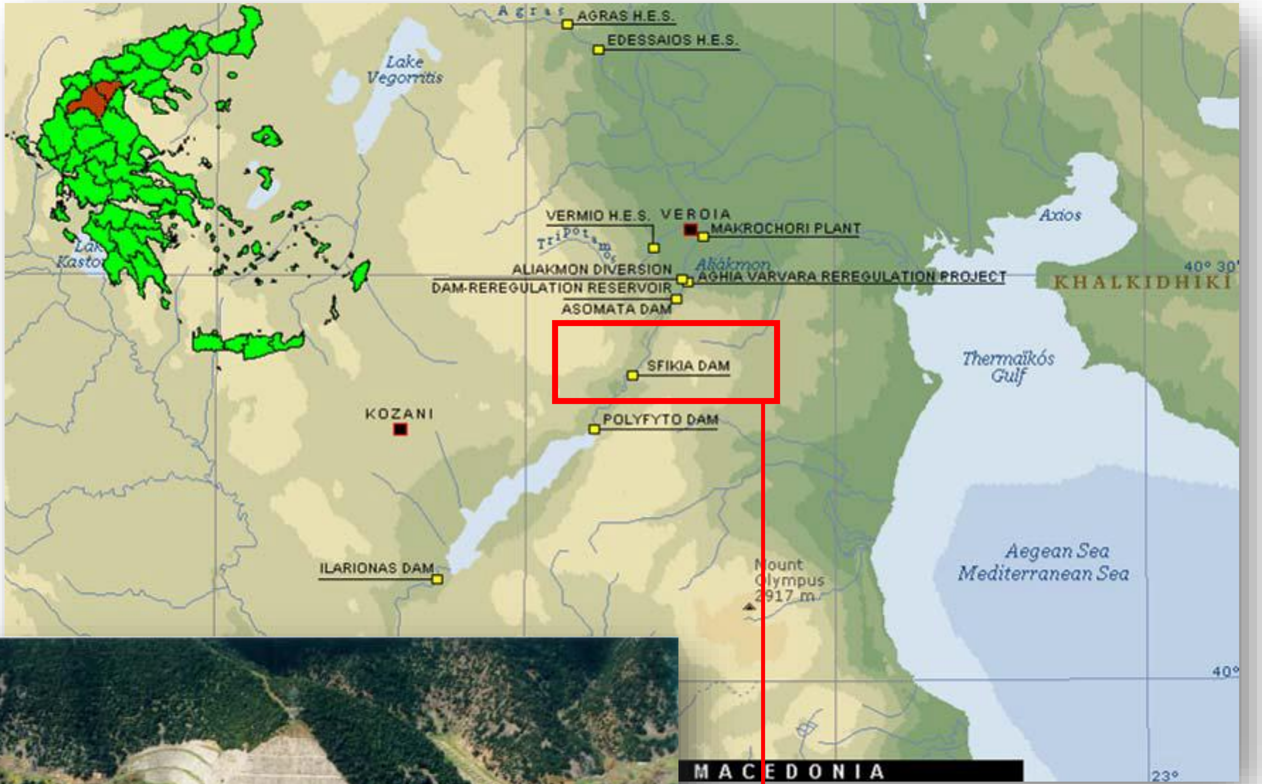

Study objective

- What **mechanisms** could cause the failure of the Brava dam (upper reservoir)?
- What are the **critical parameters and assumptions** involved in the failure of this dam, and how are they implemented in the **corresponding models**?
- How do we handle the **uncertainty of the phenomenon?**
- How is the **propagation of the flood wave represented**, and what impacts does it have along its path?
- What are the potential **adverse conditions for the Aliakmon complex?**
- What are the potential impacts of these scenarios on the **Sfikia reservoir**?
- Is there a **risk of overtopping of the Sfikia dam** and triggering of downstream cascading effects?

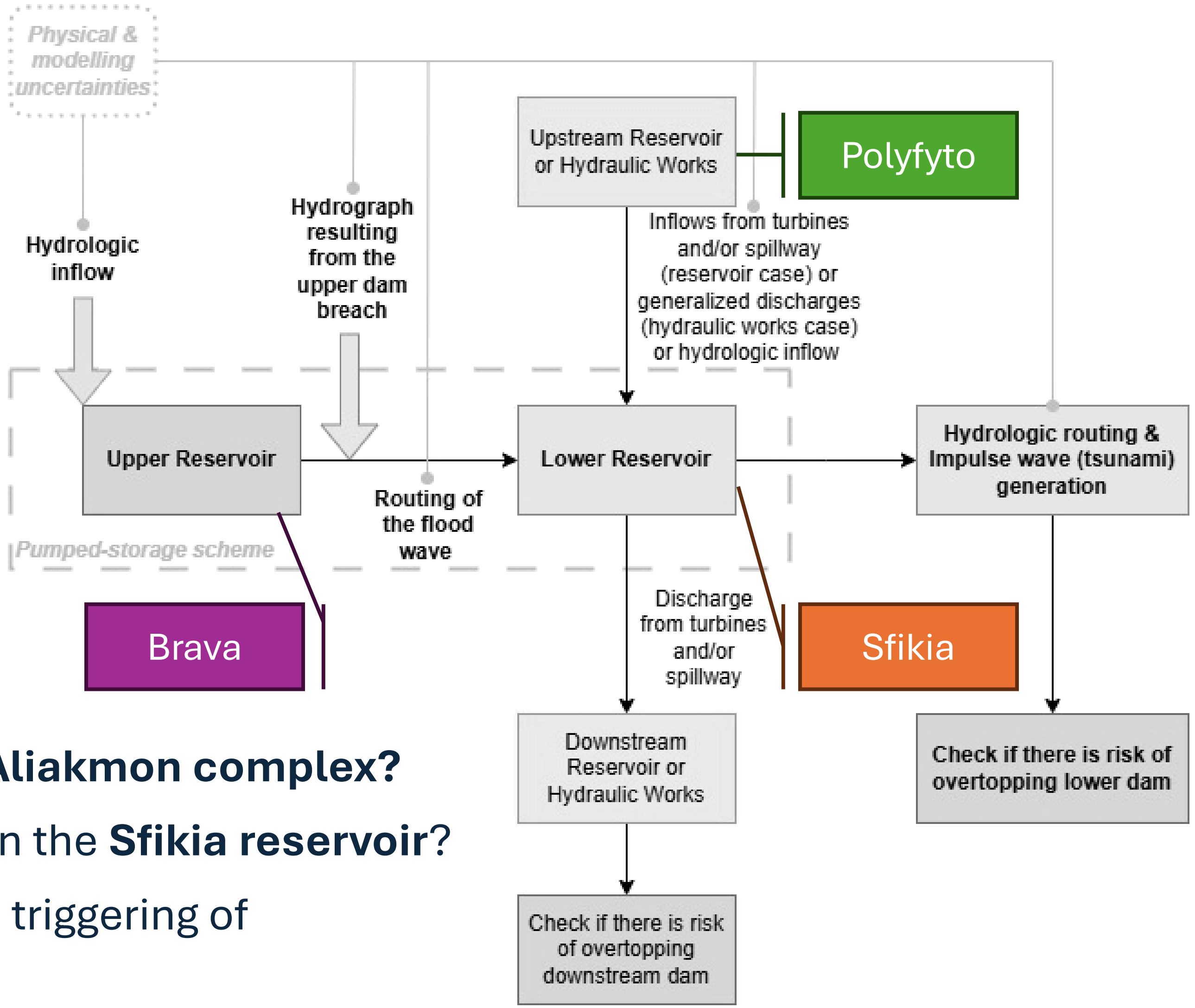

Study area - technical data (1)

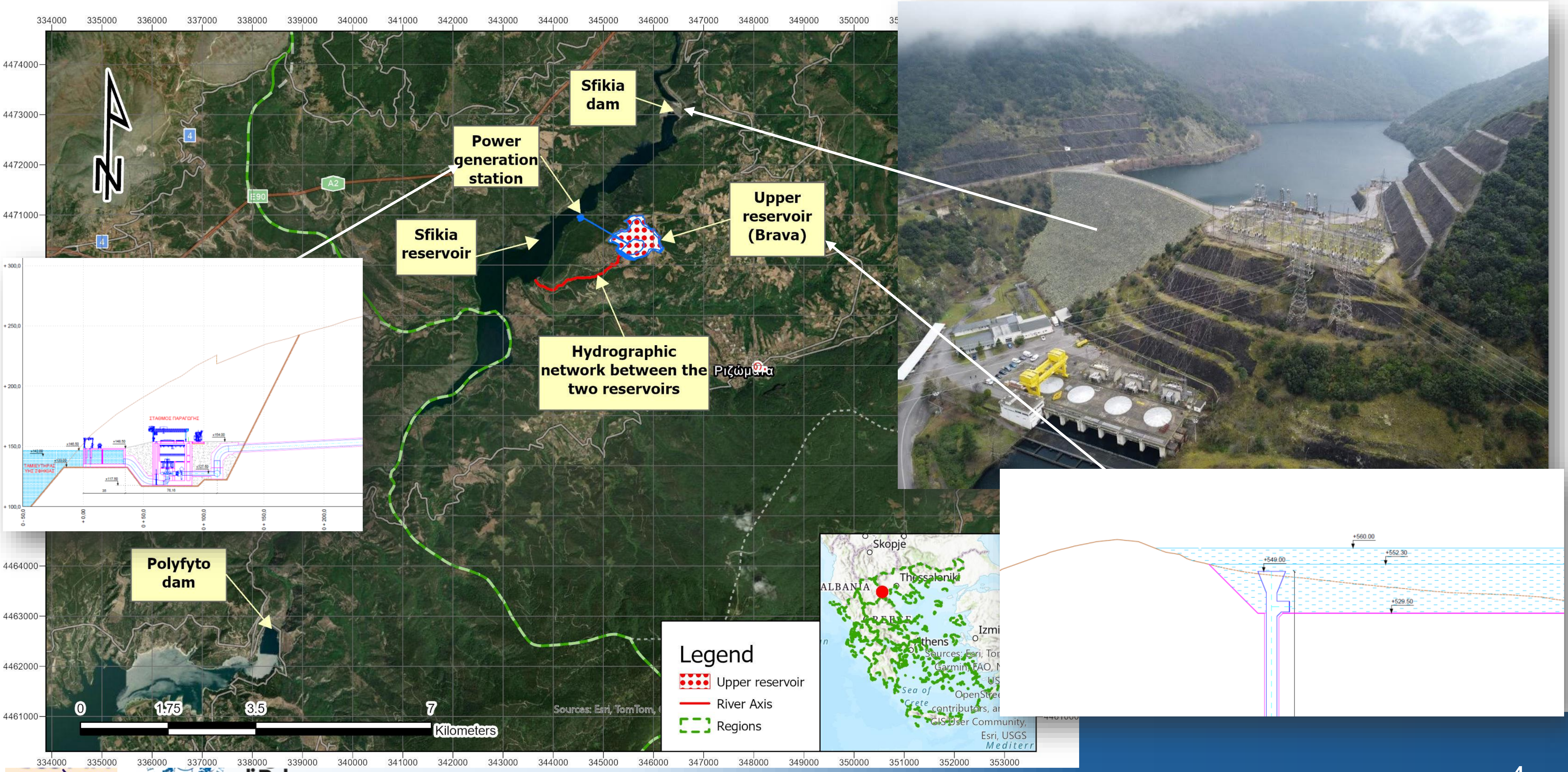

Study area - technical data (2)

A) Upstream view of the Sfikia dam

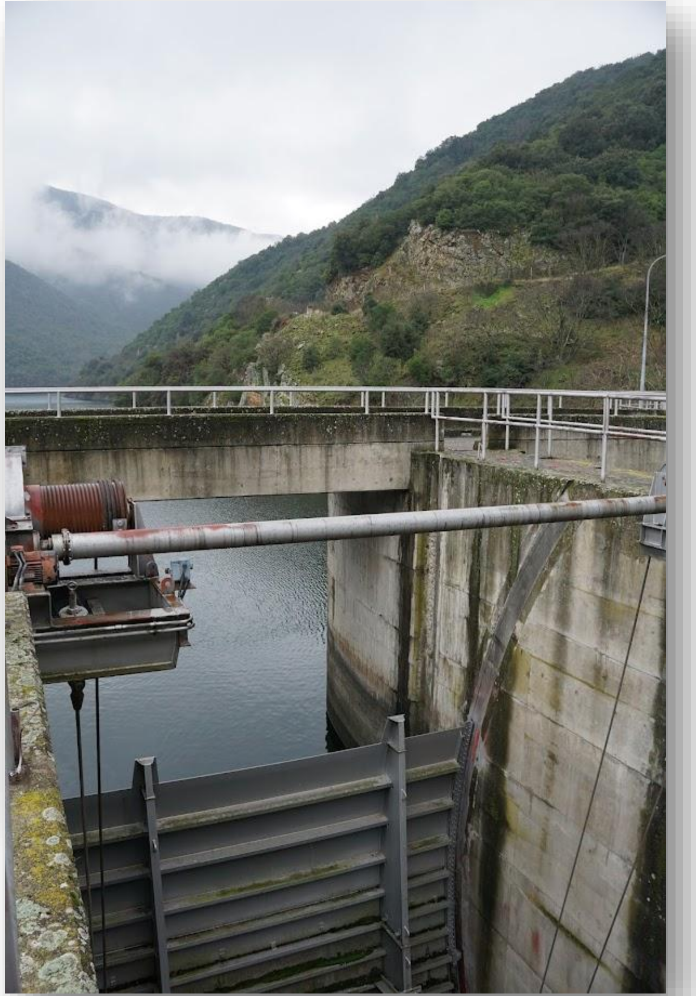

B) Spillway gates of the Sfikia dam

Investigation of dam breach scenarios: Breaching mechanisms

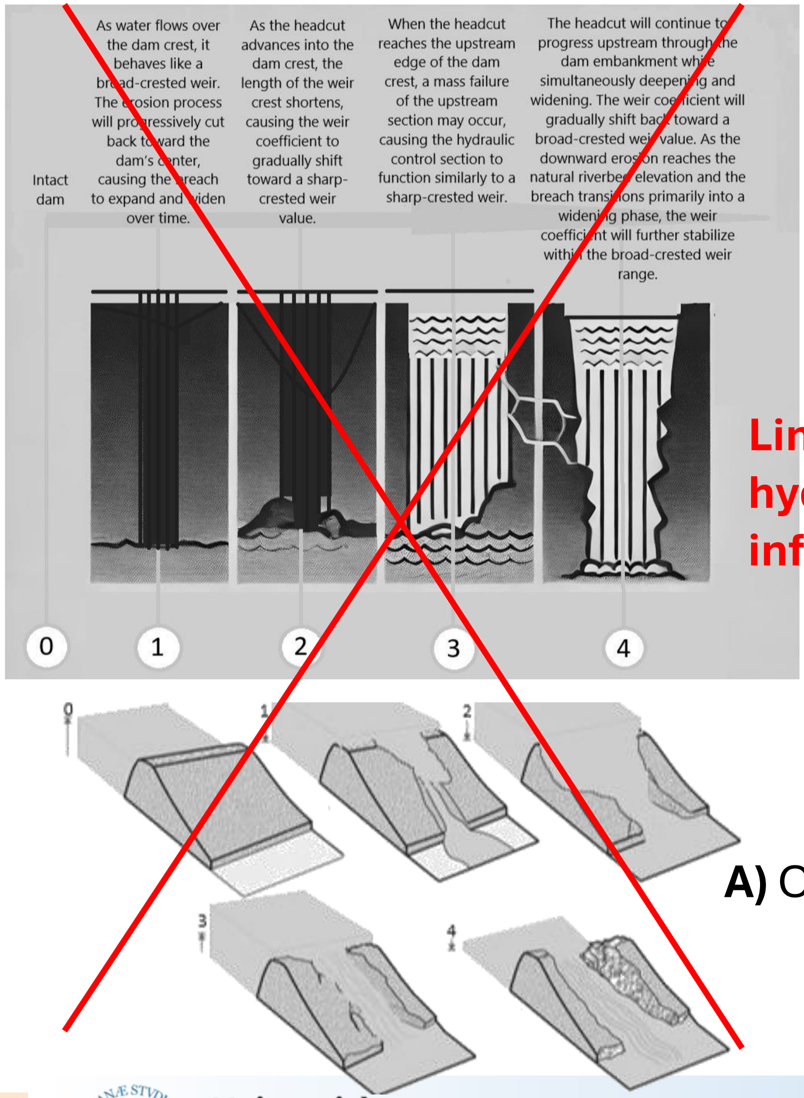

Limited hydrologic inflows

A) Overtopping

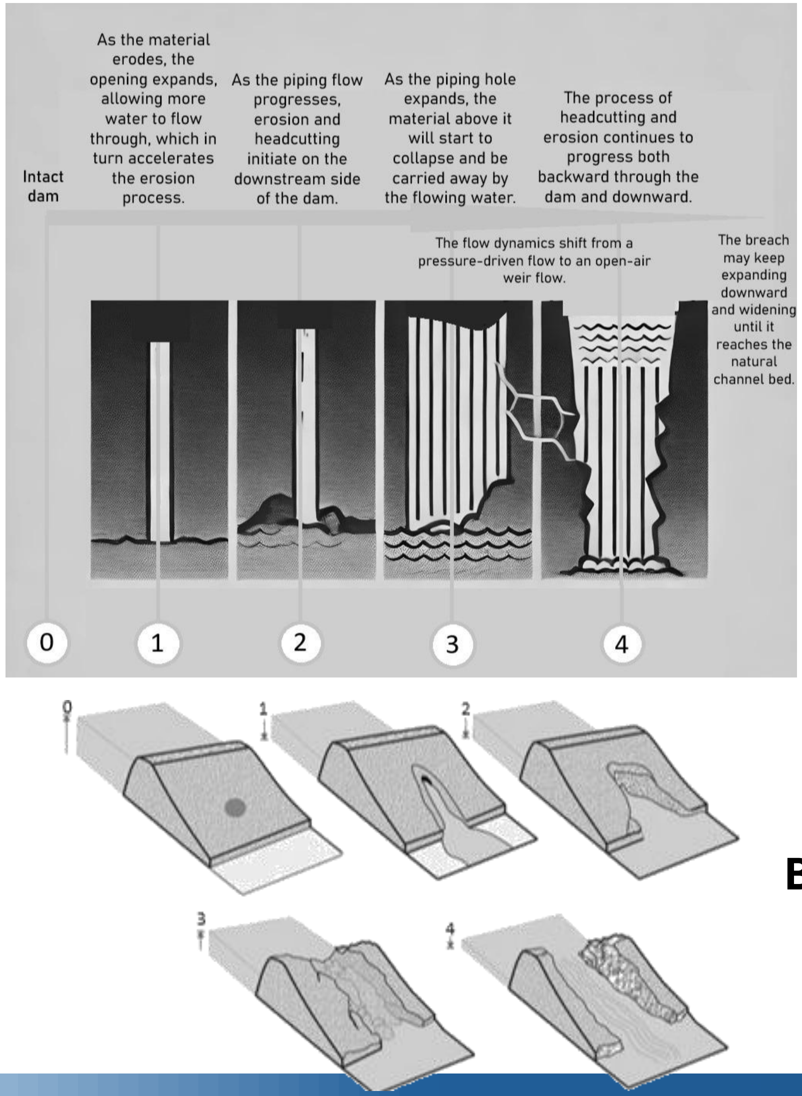

B) Piping

Investigation of dam breach scenarios: Piping scenarios

EWRA 2025

Scenario Nr.	Methodology	Final breach width (m)	Side slopes of breach (H:V)	Breach formation time (h)
1	MacDonald et al. (1984)	50	0.5	1.2
2	Froehlich (1995)	29	0.9	0.5
3	Froehlich (2008)	28	0.7	0.47
Dam erodibility		**Medium**		
4a	Von Thun and Gillette (1990)	116	0.5	0.99
5a	Xu and Zhang (2009)	28	0.6	1.32
Dam erodibility		**High**		
4b	Von Thun and Gillette (1990)	116	0.5	0.56
5b	Xu and Zhang (2009)	38	1.05	0.69

Software: BASEbreach	
Macchione (2008)	6
Peter (2017)	7
Peter Calibrated (Peter et al. 2018)	8

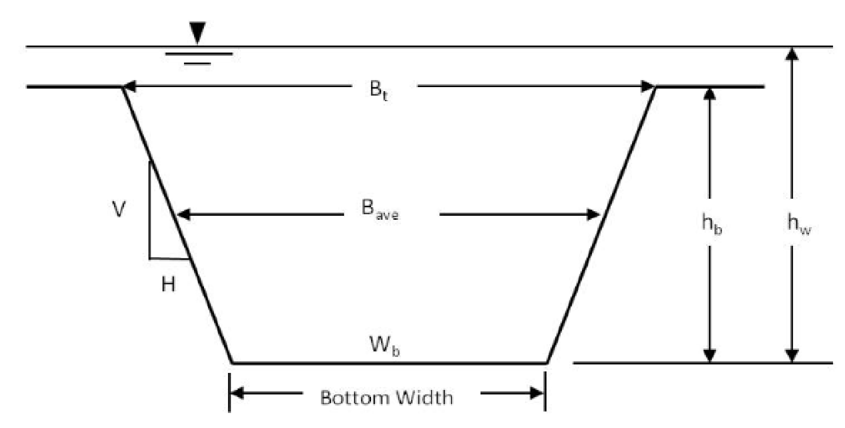

Typical breach parameters (model assumptions)

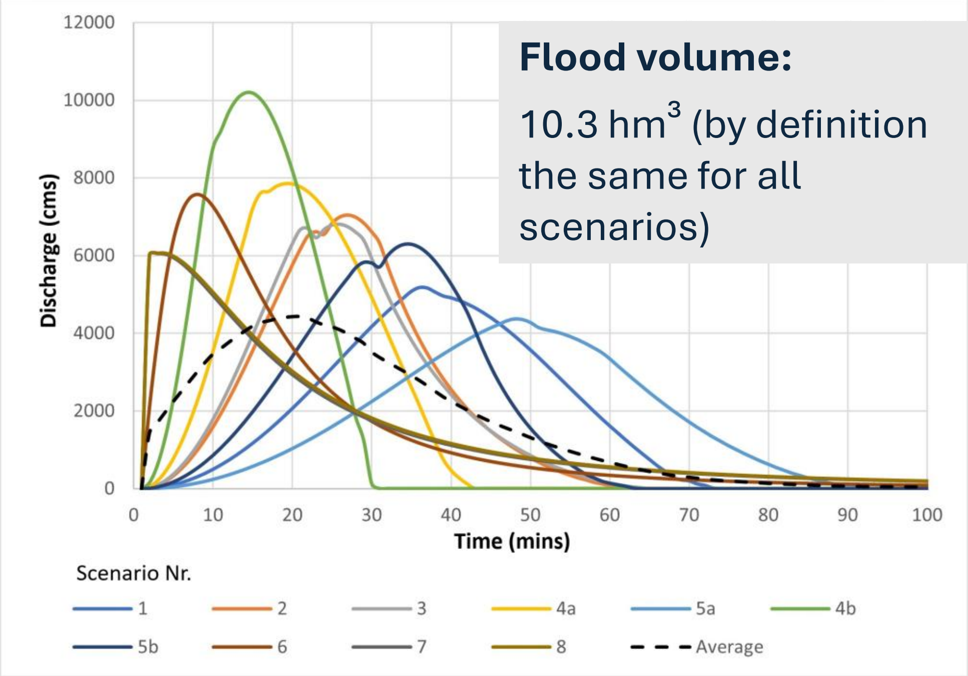

Flood volume:

10.3 hm^3 (by definition the same for all scenarios)

Ten piping scenarios are examined using different models and their respective assumptions, and the **corresponding flood hydrographs are generated** as a result of the dam failure.

EWRA

Università degli Studi di Palermo

Investigation of dam breach scenarios: Validate with empirical equations

EWRA 2025

Method	Empirical formula	Qmax (m³/s)
USBR (1982)	$Q = 19.1(h_w)^{1.85}$	15,213
MacDonald and Langridge-Monopolis (1984)	$Q = 1.154(V_w h_w)^{0.412}$	3,951
Froehlich (1995b)	$Q = 0.607{V_w}^{0.295}{h_w}^{1.24}$	6,251
Xu and Zhang (2009)	$\frac{Q}{\sqrt{g{V_w}^{5/3}}} = 0.175\left(\frac{h_d}{h_r}\right)^{0.199}\left(\frac{{V_w}^{1/3}}{h_w}\right)^{-1.274} e^{B_4}$	6,171(medium) 8,916 (high)
SCS (1981)	$Q = 16.6(h_w)^{1.85}$	13,222
Hagen (1982)	$Q = 0.54(Sh_d)^{0.5}$	10,516
Singh and Snorrason (1984) (1)	$Q = 13.4(h_d)^{1.89}$	12,969
Singh and Snorrason (1984) (2)	$Q = 1.776(S)^{0.47}$	3,503
Costa (1985) (1)	$Q = 1.122(S)^{0.57}$	12,111
Costa (1985) (2)	$Q = 0.981(Sh_d)^{0.42}$	3,978
Costa (1985) (envelope)	$Q = 2.634(Sh_d)^{0.44}$	15,865
Evans (1986)	$Q = 0.72{V_w}^{0.53}$	3,741

Parameter	Description	Value
h_w (m)	Height of water volume above the breach initiation point	37
V_w (m³)	Water volume above the breach initiation point	10.25×10^6
S (m³)	Reservoir storage above the breach initiation point	10.25×10^6
h_d (m)	Dam height	38
Parameters for the Xu and Zhang (2009) method		
h_r	Characteristic height separating large and small dams	15
b_3	Coefficient for earthen dams	-0.649
b_4	Coefficient for piping scenarios	-1.039
b_5 high	Coefficient for high erodibility	-0.007
b_5 medium	Coefficient for medium erodibility	-0.375
B_4 high	b3 + b4 + b5 high	-1.695
B_4 medium	b3 + b4 + b5 medium	-2.063

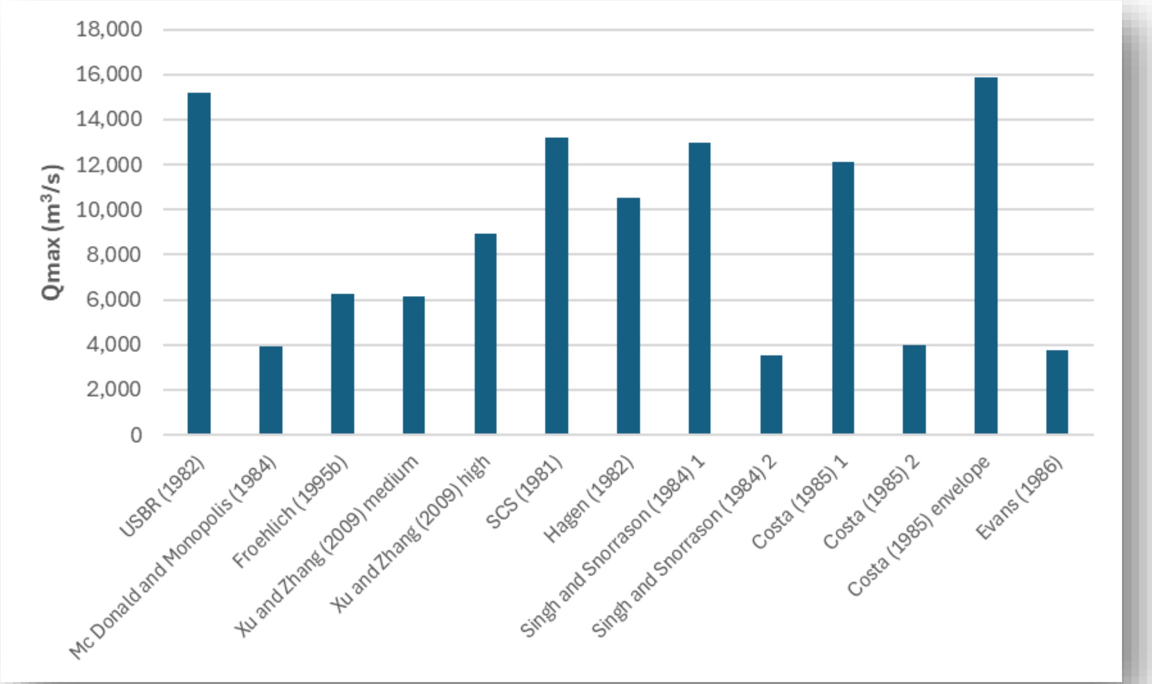

- **Flood peaks from simulation models:**
  - ❑ Average: 6,744 m³/s
  - ❑ Maximum: 10,188 m³/s
- **Flood peaks from empirical equations:**
  - ❑ Average: 7,908 m³/s
  - ❑ Maximum: 15,865 m³/s

Investigation of dam breach scenarios: Development of a representative dam-break flood hydrograph

EWRA 2025

- The scenarios reflect the high **uncertainty of the failure mechanisms**, their modeling, and the prevailing conditions.
- The objective is to develop a **representative scenario** that depicts a dam failure event of 'average' probability.
- The average of the discharge values (**mean scenario**) underestimates the peak due to the differing shapes of the individual hydrographs.
- A representative flood hydrograph is developed so as to reproduce both the **average peak flow** and the **average temporal profile** of the examined scenarios.

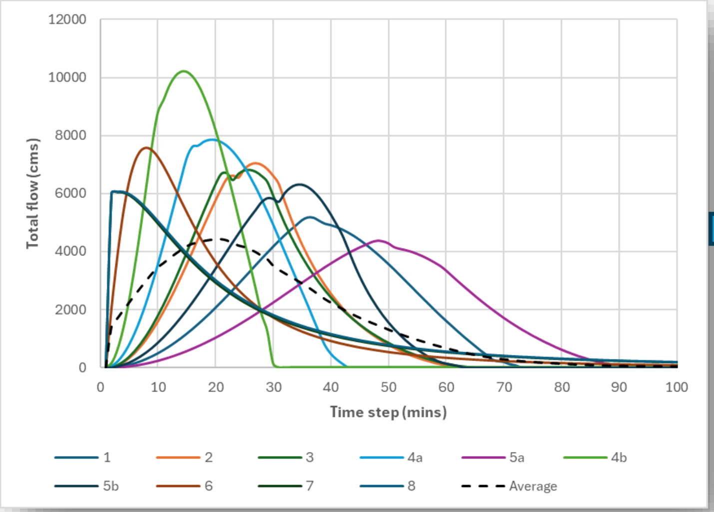

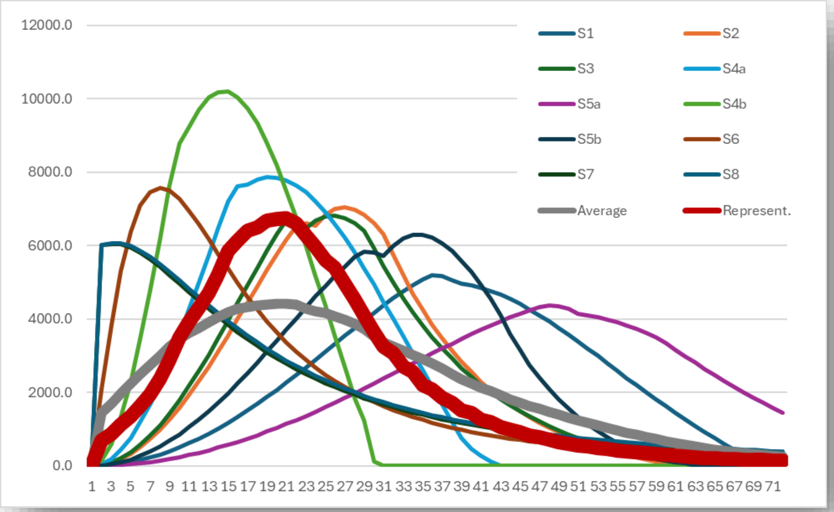

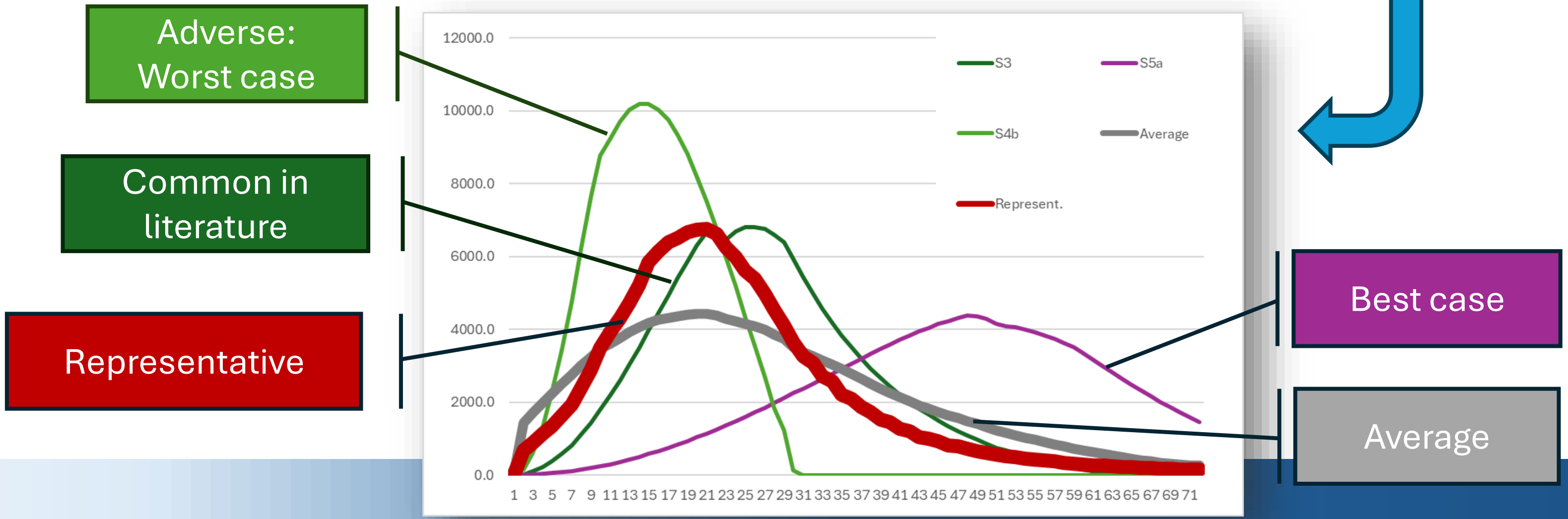

Flood wave propagation between the upper and the lower reservoir

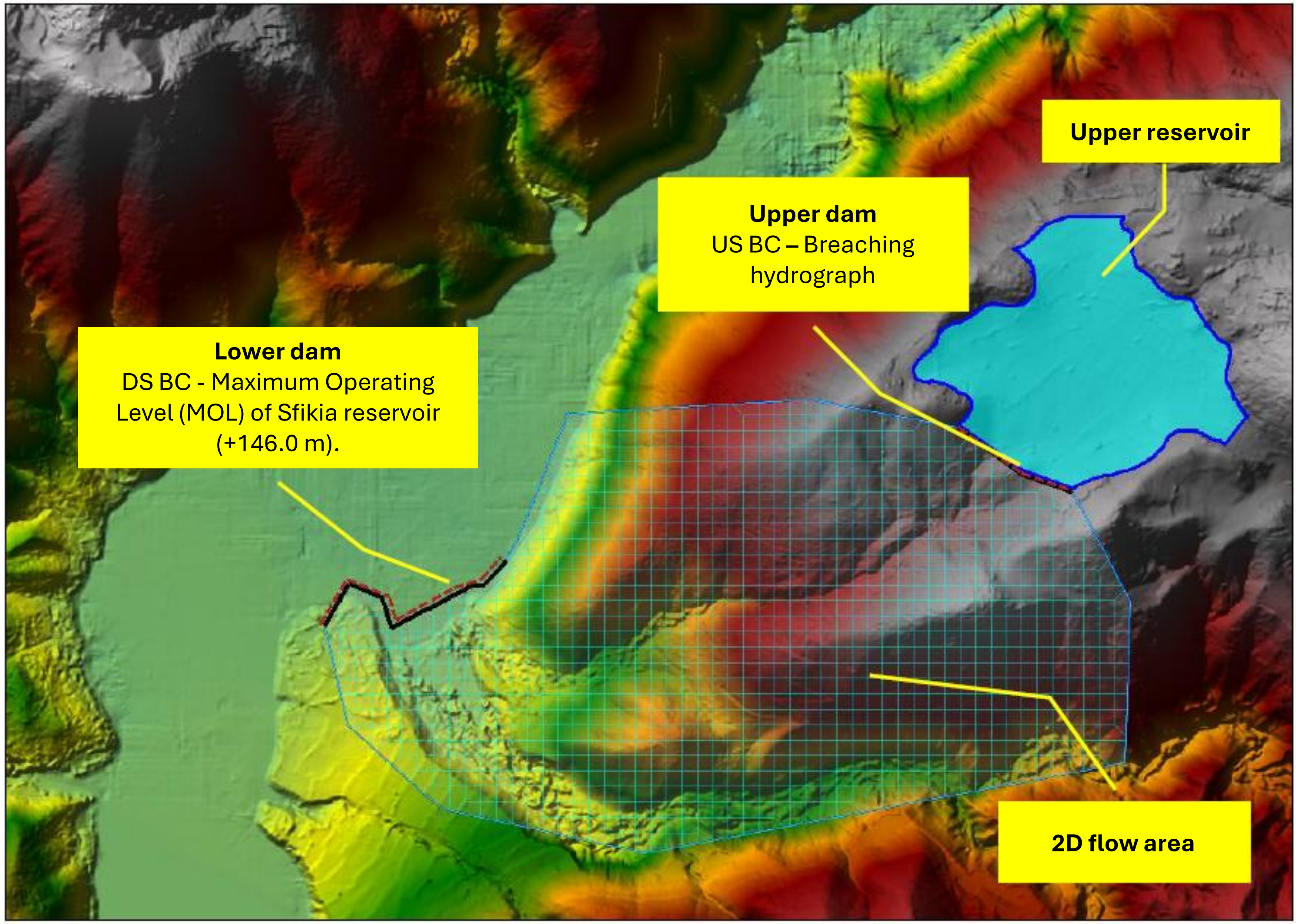

- Development of a 2D routing model using a Digital Elevation Model (DEM) with 2x2 m resolution **from the Cadastre**.
- The model was developed in the **HEC-RAS software** by the US Army Corps of Engineers, specifically in its latest version (6.6).
- Key model **assumptions**:
  - Element **discretization**: 50 x 50 m
  - **Time step**: 1.0 s (CFL criterion)
  - **Manning's n** = 0.06
  - **Upstream boundary condition**: dam-break hydrograph
  - **Downstream boundary condition**: Sfikia Reservoir Water Surface Elevation (+146.00)

Flood wave propagation between the upper and the lower reservoir: Results

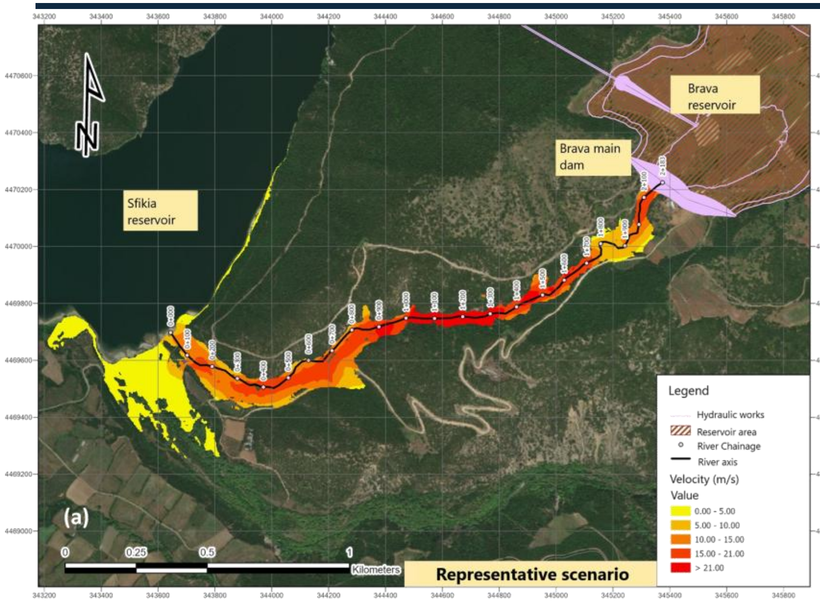

A) Maximum velocity

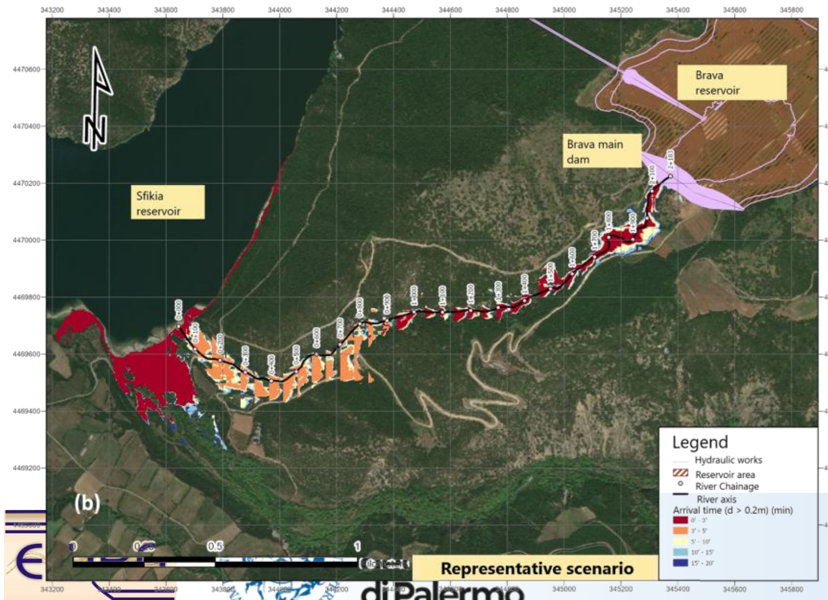

B) Arrival time

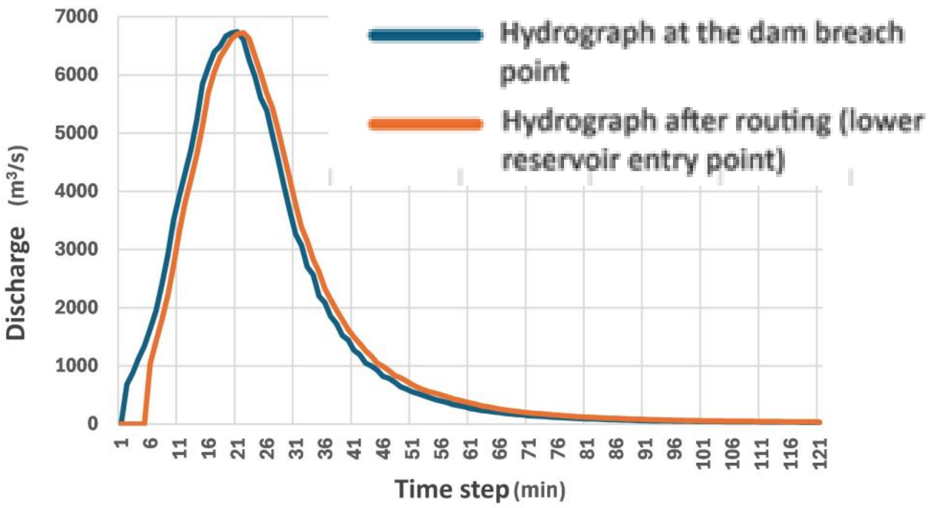

Comparison of upstream and downstream hydrographs and volumes:

- Steep terrain slopes → short lag time (~5 min) → **limited peak attenuation** (adverse: 0.2%, best case: 0.4%, representative: 0.2%)
- The corresponding **flood volumes** range from 6.9 to 8.3 hm^3 (volume released during the dam break: 10.5 hm^3)

Routing of the flood hydrograph in the downstream reservoir

- **4 scenarios -** Aliakmon Hydropower Complex: Combination of **2 upstream dam breach hydrographs** (representative & adverse) with **2 operational modes** of the complex

- **Idle Mode**:
  - ❑ No flow between reservoirs (Polyfyto → Sfikia → Asomata)
  - ❑ All structures initially closed
  - ❑ Turbines (600 m³/s) fully operational after 10 min
  - ❑ Spillway gates (up to 1600 m³/s) open gradually over 30 min
- **Flood Design Mode**:
  - ❑ Full operational capacity across all facilities
  - ❑ Constant inflow to Sfikia: **1,720 m³/s**
  - ❑ Outflow via turbines: **600 m³/s** + fully open spillway

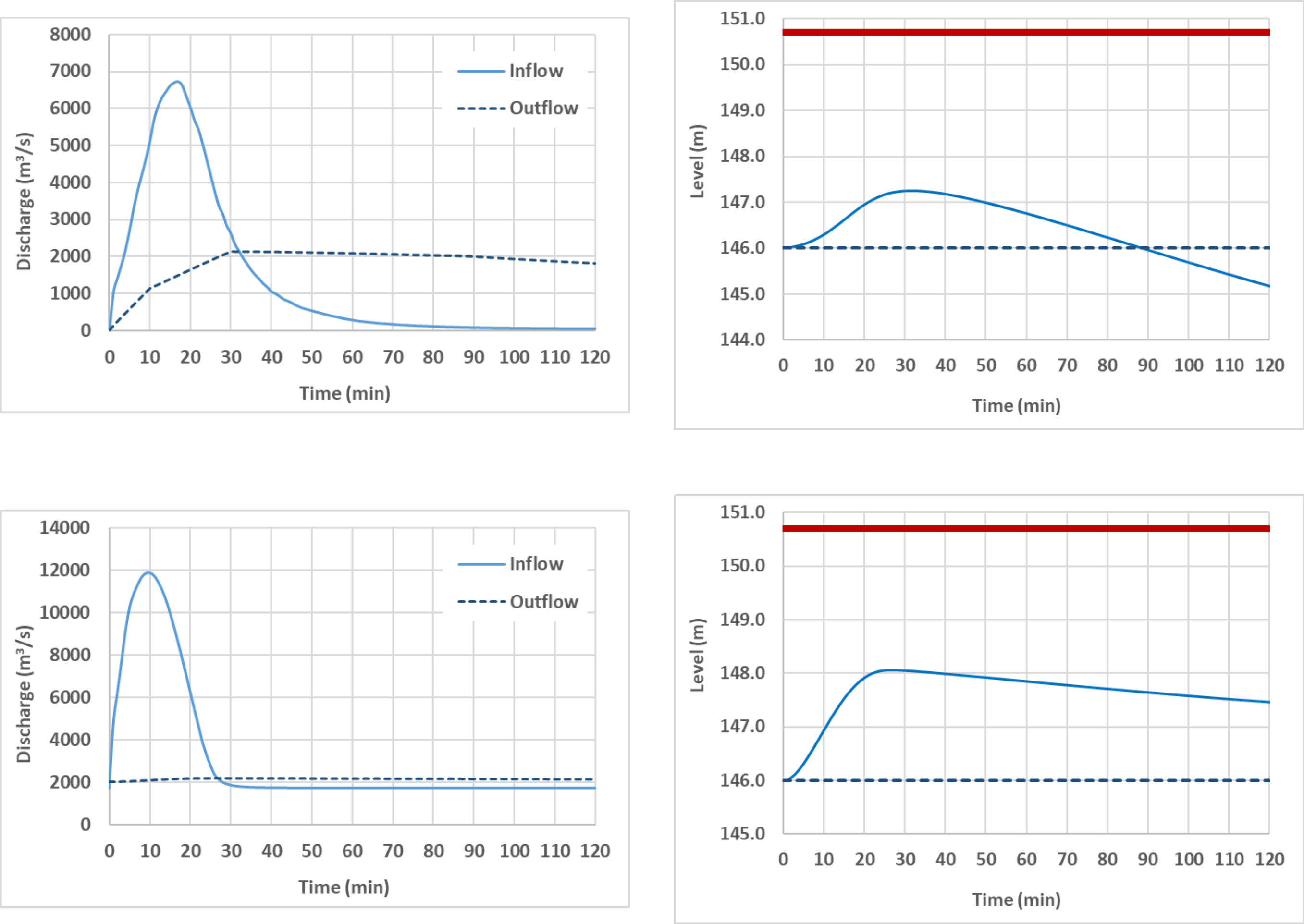

Time series of inflows vs. routed outflows (left) and reservoir level (right) for scenarios 1 (upper panel) and 4 (lower panel). The red line indicates the dam crest.

Impulse wave/tsunami generation: Theoretical approach

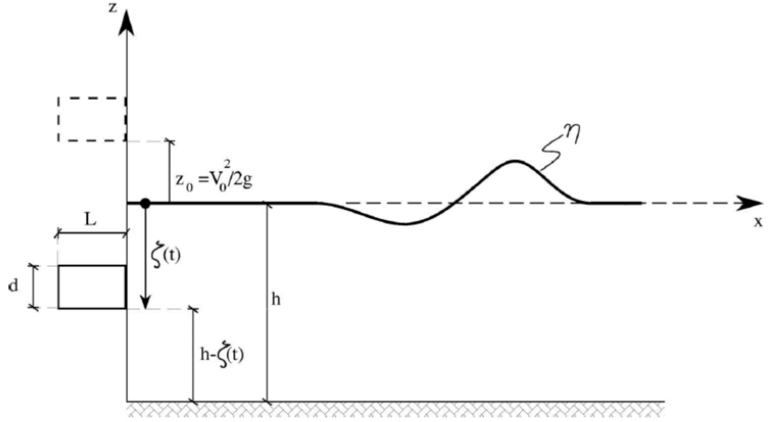

- Simulation of wave generation from the landslide.
- Wave attenuation due to *bottom friction, radial dispersion, and diffraction:*

$$n(x,t) = 2\frac{P}{\rho\beta(t)}\sqrt{\frac{h}{g}}\left\{A_i[Z(x+L,t)] - A_i\left[Z(x+L,t)+\frac{L}{\beta(t)}\right]\right\} + \int_0^{t_{imm}}\frac{LV(\tau)}{\beta(t-\tau)}A_i[Z(x,t-\tau)]d\tau + \frac{P}{\rho}\int_0^{t}\frac{1}{\beta(\tau)}\frac{1}{\beta(t-\tau)}A_i[Z(x,t-\tau)]\{A_i[Z(2L,\tau)] + A_i[Z(0,\tau)]\}d\tau$$

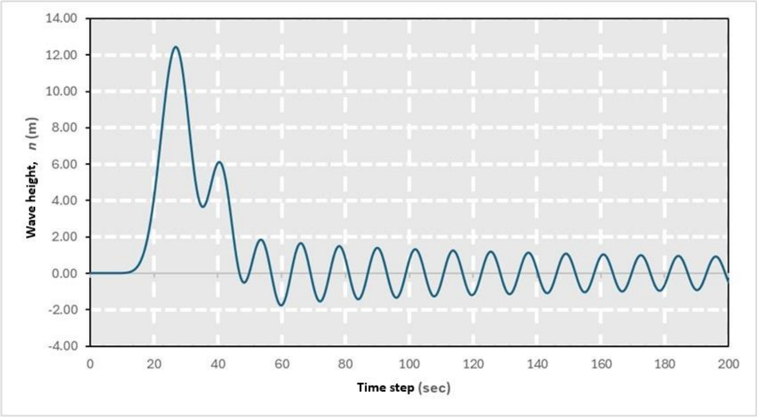

Results of wave height differential equation solution.

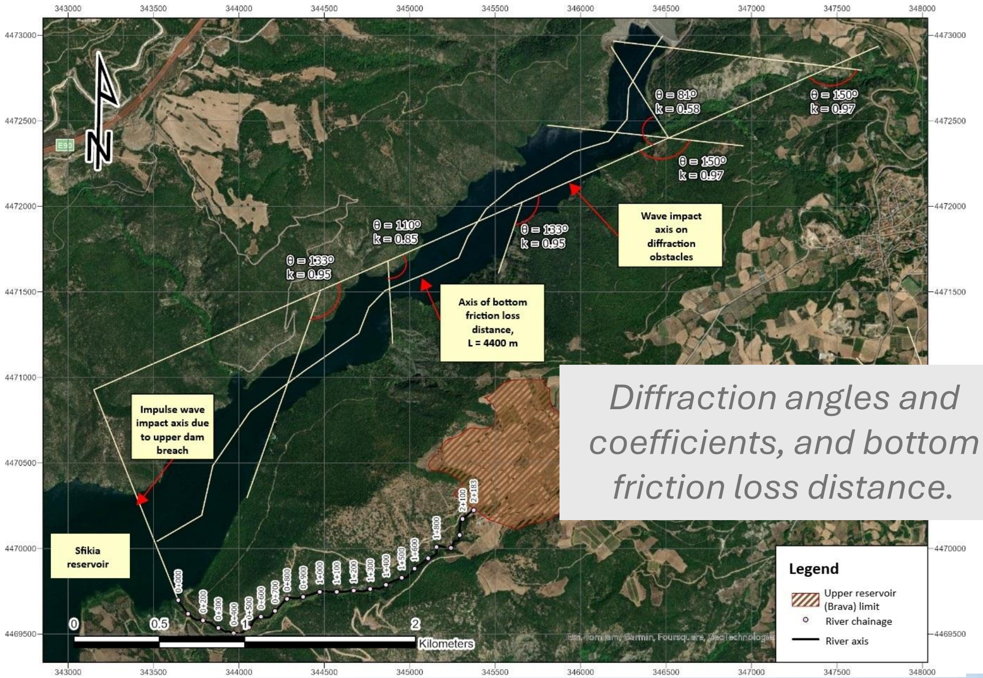

Diffraction angles and coefficients, and bottom friction loss distance.

Bottom friction coefficient, f_w	Initial wave height at the dam (m)	Wave height after diffraction (m)	Run-up, R (m)	Maximum water level (m)	Distance from dam crest (m)
0.05	3.5	1.5	3.7	149.7	1.0
0.50	1.9	0.8	2.0	148.0	2.7
1.00	1.3	0.5	1.4	147.4	3.3

Key results of theoretical analysis for three bottom friction coefficient values.

$$R = 2\ a\ exp(0.4\varepsilon)\left(\frac{90^0}{\beta}\right)^{0.20}$$

Impulse wave/tsunami generation: Semi-empirical approach (1/2)

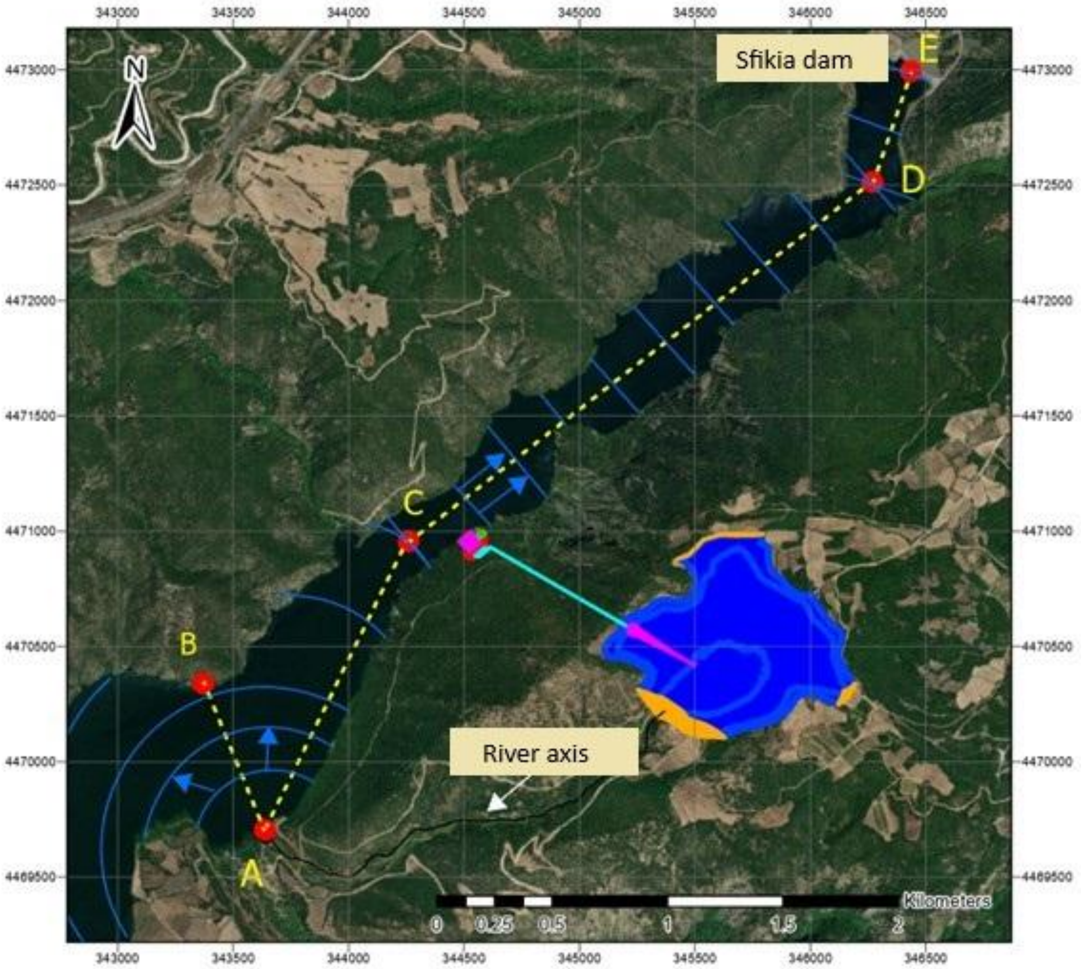

Geometry of Sfikia reservoir and characteristics points illustrating the route of the wave produced by the water volume arriving at point A

- Application of the methodology proposed by the **Laboratory of Hydraulics, Hydrology and Glaciology of ETH Zurich** (Evers et al., 2019).
- Use of **empirical relationships** for the estimation of wave generation, propagation (2D/3D), and run-up calculation.
- Part of the computational process is supported **by a tool implemented in Excel**, available at https://zenodo.org/records/3492000

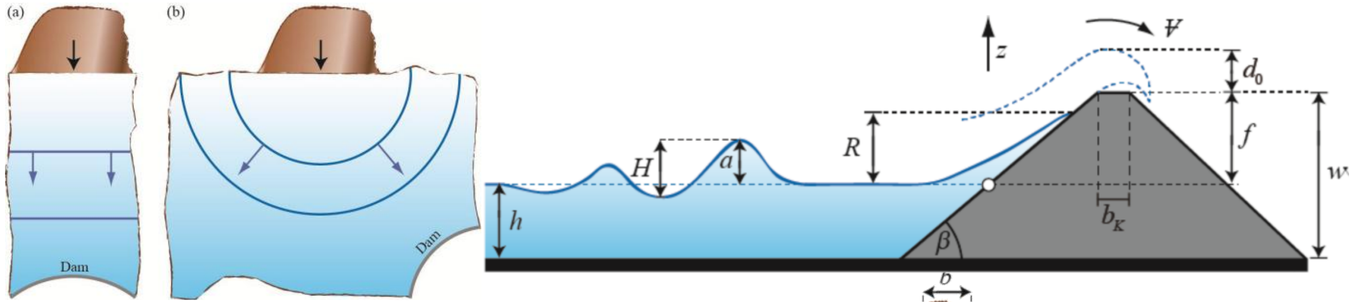

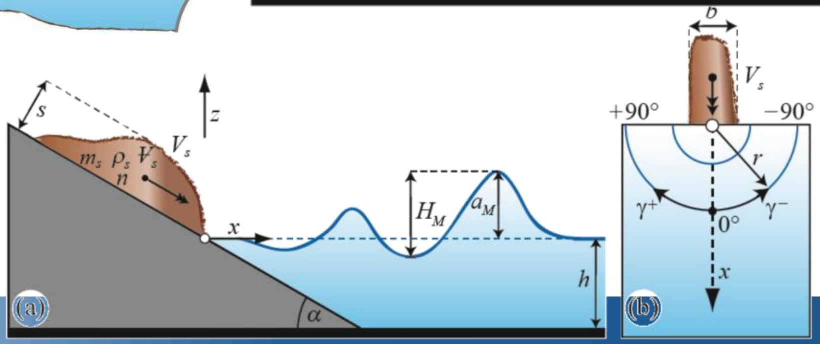

Impulse wave/tsunami generation: Semi-empirical approach (2/2)

EWRA 2025

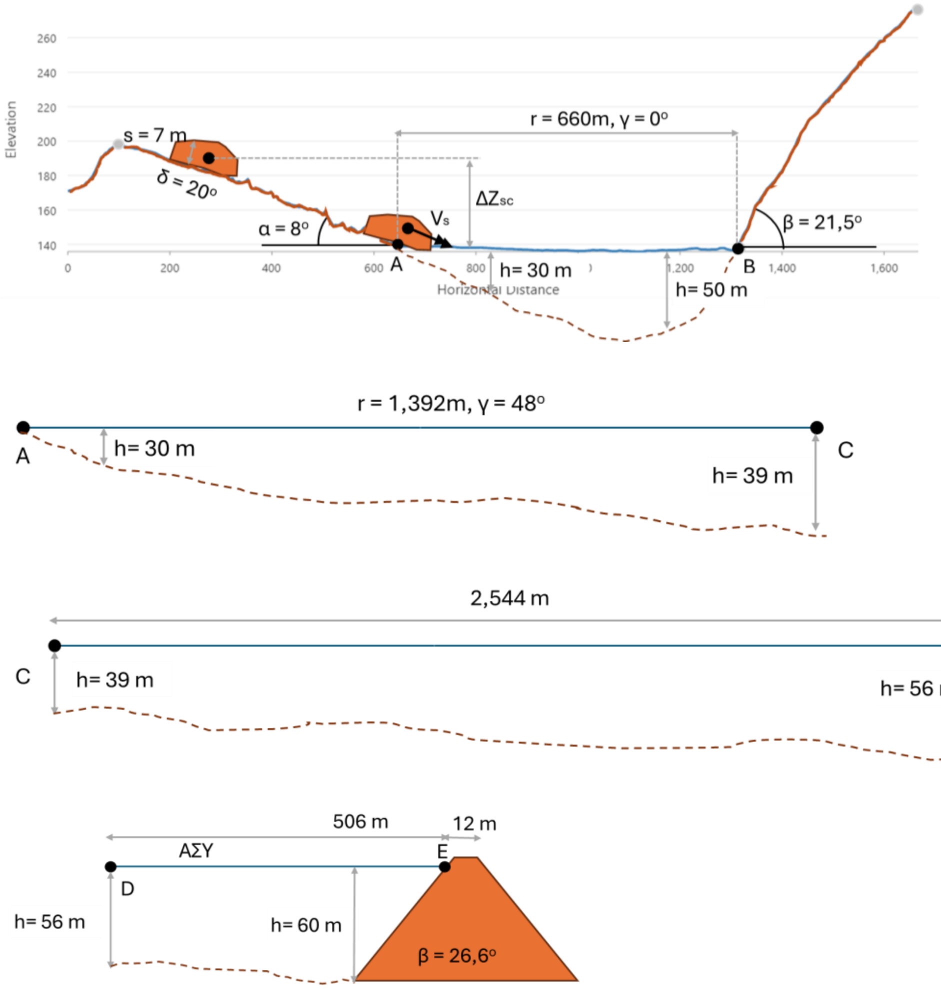

Layout of cross-sections AB, AC, CD, and DE (from top to bottom).

- **Significant wave attenuation** observed along the propagation path due to **radial dispersion** and **bottom friction.**
- **Wave crest amplitudes** at key locations:
  - ❑ **Location B** (660 m, 0° angle): 6.4 m
  - ❑ **Location C** (1392 m, 48° angle): 1.9 m
  - ❑ **Location E** (dam site, 4440 m): 0.55 m
- **Wave run-up (R)** estimates:
  - ❑ **Location B**: ~18 m
  - ❑ **Location E**: ~1.41 m
- Consistent with the theoretical scenario
- **Wave arrival times** at critical points:
  - ❑ From **Location A to B**: 31 seconds
  - ❑ From **A to dam (E)**: 208 seconds
- Much **earlier than the peak** of the routed flood hydrograph (~27 minutes)
- **Critical implications avoided**:
  - ❑ **Potential overlap** of tsunami and routed flood peaks could **trigger overtopping** at Sfikia Dam
  - ❑ **Risk of cascading failures** in the downstream hydrosystem

EWRA

Università degli Studi di Palermo

Conclusions

- **Exploration of multiple failure scenarios** and identification of a **representative flood hydrograph**.
- **2D hydrodynamic flow simulation** for the **favorable**, **adverse**, and **representative** scenarios.
- **Assessment of impacts on the Sfikia reservoir**:
  a) Routing of flood discharges through hydraulic structures (under various operational conditions of Polyfyto and Sfikia),
  b) Tsunami-like wave generation and propagation.
- **No overtopping risk** for Sfikia dam from routed flood peaks:
  - Maximum water level rises **2.3 m above normal operating level** and **remains 2.4 m below the dam crest** in the worst-case scenario.
- **Tsunami-induced run-up** estimated between **1.4 and 3.7 m**, leaving a **safety margin** of **3.3 to 1.0 m** below the dam crest (**significant uncertainties** due to the **high complexity** of the hydrodynamic problem).
- The two processes **do not coincide in time**: **Flood peak** occurs ~30 min after breach, **Tsunami wave** reaches the dam in ~3–5 minutes.
- **Need for the preparation of measures**:
  a) Maintenance and monitoring.
  b) Preparedness and training.
  c) Emergency Action Plan (EAP) *by the* ***General Secretariat for Civil Protection*** *in collaboration with* ***Public Power Corporation S.A. (PPC S.A.)***

References

i. Ackerman, C. T., M. J. Fleming, and G. W. Brunner (2008). Hydrologic and hydraulic models for performing dam break studies. In *World Environmental and Water Resources Congress 2008*, 1–11. Honolulu, Hawaii, United States: American Society of Civil Engineers. doi:10.1061/40976(316)285.

ii. Albu, L.-M., A. Enea, M. Iosub, and I.-G. Breabăn (2020). Dam breach size comparison for flood simulations: A HEC-RAS based, GIS approach for Drăcșani Lake, Sitna River, Romania. *Water*, 12(4), 1090. doi:10.3390/w12041090.

iii. Amini, A., J. Bahrami, and A. Miraki (2022). Effects of dam break on downstream dam and lands using GIS and HEC RAS: A decision basis for the safe operation of two successive dams. *International Journal of River Basin Management*, 20(4), 487–498. doi:10.1080/15715124.2021.1901728.

iv. Butt, M. J., M. Umar, and R. Qamar (2013). Landslide dam and subsequent dam-break flood estimation using HEC-RAS model in Northern Pakistan. *Natural Hazards*, 65(1), 241–54. doi:10.1007/s11069-012-0361-8.

v. Dean, R. G., and R. A Dalrymple (1991). *Water Wave Mechanics for Engineers and Scientists*. Vol. 2. *World Scientific Publishing Company*.

vi. Di Risio, Marcello, and Paolo Sammarco (2008). Analytical Modeling of Landslide-Generated Waves. *Journal of Waterway, Port, Coastal, and Ocean Engineering* 134 (1): 53–60.

vii. Dyer, K. R. (1986). *Coastal and Estuarine Sediment Dynamics*.

viii. Efstratiadis, A., I. Tsoukalas, D. Koutsoyiannis (2021). Generalized storage-reliability-yield framework for hydroelectric reservoirs. *Hydrological Sciences Journal*, 66(4), 580–599, doi:10.1080/02626667.2021.1886299.

ix. Evers, F. M. (2019). Computational tool for “Landslide-generated Impulse Waves in Reservoirs – Basics and Computation” (1.0). Zenodo. doi:10.5281/zenodo.3492000

x. Evers, F. M., V. Heller, H. Fuchs, W.H. Hager, and R.M. Boes (2009). Landslide-generated Impulse waves in reservoirs: Basics and computation. Mitteilungen 211, *Versuchsanstalt für Wasserbau, Hydrologie und Glaziologie (VAW)*, R. Boes, Hrsg., ETH Züri

xi. Goda, Y. (2010). *Random Seas and Design of Maritime Structures*. World Scientific.

xii. Goodell, C. R. (2005). Dam break modeling for Tandem reservoirs — A case study using HEC-RAS and HEC-HMS. In *Impacts of Global Climate Change*, 1–11. Anchorage, Alaska, United States: American Society of Civil Engineers. doi:10.1061/40792(173)402.

xiii. Hardisty, J. (1990). *Beaches: Form and Process*. Springer Science & Business Media.

xiv. Howarth, L. (1979). One hundred years of Lamb’s Hydrodynamics. *Journal of Fluid Mechanics*, 90(1), 202–207.

xv. Institut de Mécanique des Fluides de Toulouse (1977). Rapport No 328-9, Toulouse.

EWRA 2025

URBAN WATER
MANAGEMENT AND
HYDROINFORMATICS
GROUP

Thank you!

EWRA

Università
degli Studi
di Palermo